Hydrolysis of Angiotensin II Receptor Blocker Prodrug Olmesartan Medoxomil by Human Serum Albumin and Identification of Its Catalytic Active Sites

Shen-Feng Ma, Makoto Anraku, Yasunori Iwao, Keishi Yamasaki, Ulrich Kragh-Hansen, Noriyuki Yamaotsu, Shuichi Hirono, Toshihiko Ikeda, and Masaki Otagiri.

Graduate School of Pharmaceutical Sciences, Kumamoto University, Kumamoto 862-0793, Japan (S.-F. M., M. A., Y. I. and M. O.).

Department of Pharmacy, Miyazaki Medical College Hospital, Miyazaki 889-1692, Japan (K. Y.).

Department of Medical Biochemistry, University of Aarhus, DK-8000 Aarhus C, Denmark (U. K.-H.).

The School of Pharmaceutical Sciences, Kitasato University, Tokyo 108-8641, Japan (N. Y. and S. H.).

Drug Metabolism and Pharmacokinetics Research Laboratories, Sankyo Co., Ltd., Tokyo 140-8710, Japan (T. I.).

a) **Running Title:** Hydrolysis of CS-866 by HSA and studies of the active sites

b) **Corresponding author:** Professor Masaki Otagiri, Ph.D.,

Department of Biopharmaceutics, Graduate School of Pharmaceutical Sciences, Kumamoto University, 5-1 Oe-honmachi, Kumamoto 862-0973, Japan

Tel: +81-96-371-4150; Fax: +81-96-362-7690

E-mail: otagirim@gpo.kumamoto-u.ac.jp

c) Number of text pages: 29

Number of figures: 7

Number of tables: 5

Number of references: 34

Number of words in the Abstract: 233

Number of words in the Introduction: 382

Number of words in the Discussion: 1465

d) **Abbreviations used:** PNPA, p-nitrophenyl acetate; n-butyl-p-AB, n-butyl-p-aminobenzoate.

DMD Fast Forward. Published on September 23, 2005 as DOI: 10.1124/dmd.105.006163
This article has not been copyedited and formatted. The final version may differ from this version.

Abstract

In the present study, we investigated the esterase-like activity of human serum albumin (HSA) and the mechanism by which it hydrolyzes, and thereby activates, olmesartan medoxomil (CS-866), a novel angiotensin II receptor antagonist. CS-866 has previously been shown to be rapidly hydrolyzed in serum in which HSA appeared to play the most important role in catalyzing the hydrolysis. We found that the hydrolysis of CS-866 by HSA followed Michaelis-Menten kinetics. Compared with the release of *p*-nitrophenol from *p*-nitrophenyl acetate (PNPA), CS-866 showed lower affinity to HSA and a lower catalytic rate of hydrolysis. Thermodynamic data indicated that PNPA has a smaller value of activation entropy (ΔS) than CS-866; consequently, PNPA is more reactive than CS-866. Ibuprofen and warfarin acted as competitive inhibitors of hydrolysis of CS-866, whereas Dansyl-L-asparagine (DNSA), n-butyl *p*-aminobenzoate (n-butyl *p*-AB) and diazepam did not. These findings suggest that the hydrolytic activity is associated to parts of site I and site II for ligand binding. All chemically modified HSA derivatives (Tyr-, Lys-, His- and Trp-modifications) had significantly lower reactivity than native HSA; Lys-HSA and Trp-HSA had especially low reactivity. All the mutant HSAs tested (K199A, W214A and Y411A) exhibited a significant decrease in reactivity, suggesting that Lys-199, Trp-214 and Tyr-411 play important roles in the hydrolysis. Results obtained using a computer docking model are in agreement with the experimental results, and strongly support the hypotheses that we derived from the experiments.

Introduction

Ester prodrugs are hydrolyzed to their pharmacologically active metabolites after absorption. Esterases present in the small intestine, plasma and liver are involved in this process. In most cases, intestinal esterases serve as the major enzymes in activation of prodrugs during the first pass through the gut after absorption. However, prodrugs that are relatively resistant to hydrolysis by intestinal esterases enter the blood circulation, and are activated by serum (plasma) and liver esterases. The major hydrolyzing enzymes in serum are cholinesterase, arylesterase, carboxylesterase and albumin. The relative importance of each serum esterase in prodrug activation varies among animal species and prodrugs.

Olmesartan medoxomil (CS-866: (5-methyl-2-oxo-1, 3-dioxolen-4-yl) methoxy-4-(1-hydroxyl-1-methylethyl)-2-propyl-1-{4-[2-(tetrazol-5-yl)-phenyl]phenyl}methylimidazol-5-carboxylate) is a novel nonpeptide angiotensin II receptor antagonist that acts as an antihypertensive prodrug (Neutel, 2001; Koike et al., 2001; Brousil and Burke, 2003). After oral administration, CS-866 is rapidly de-esterified, producing an active acid metabolite, olmesartan (RNH-6270) (Fig. 1) (Neutel, 2001; Koike et al., 2001; Brousil and Burke, 2003). Hydrolysis of CS-866 in serum has been observed in several species, and comparison between 5 species has shown that hydrolytic activity is highest in rabbits, followed by dogs, mice, rats and humans (Ikeda, 2000). Furthermore, it was found that differences in hydrolytic activity due to serum albumin are large compared to the combined activity of all serum components. Thus, HSA might make an important contribution to activation of CS-866 after oral administration.

In the present study, we examined the esterase-like activity of HSA and the mechanism of its hydrolysis of CS-866. First, the general properties of the hydrolytic

reaction of HSA with CS-866 were determined, including the kinetics and thermodynamics, and compared with those of the hydrolytic reaction between HSA and *p*-nitrophenyl acetate (PNPA) (Means and Bender, 1975; Sakurai et al., 2004). Second, to characterize the effects of exogenous compounds on hydrolysis, we investigated changes in hydrolytic activity in the presence and absence of various ligands. Then, we examined the importance of certain types of amino acid residues of HSA for the hydrolysis of CS-866, using chemical modification techniques. Recombinant HSA (rHSA) proteins with alterations of specific amino acid residues were prepared using site-directed mutagenesis techniques, to obtain detailed information about the contribution of those residues. Finally, computer docking models of CS-866 and HSA were constructed and were found to be consistent with the experimental results.

Materials and Methods

Materials

HSA was donated by the Chemo-Sera-Therapeutic Research Institute (Kumamoto, Japan). HSA was defatted before use (Chen, 1967).

CS-866 and RNH-6270 were donated by Sankyo Co., Ltd. (Tokyo, Japan). PNPA, succinic anhydride (SA) and n-butyl *p*-aminobenzoate (n-butyl *p*-AB) were purchased form Nakalai Tesque (Kyoto, Japan). Warfarin was obtained from Eisai Co., Tokyo, Japan; ibuprofen was obtained from Kaken Pharmaceutical Co., Osaka, Japan; diazepam was obtained from Sumitomo Pharmaceutical Co., Osaka, Japan; tetranitromethane (TNM) was obtained from Aldrich Chemical Company, Inc. U.S.A.; and trinitrobenzensulfonic acid (TNBS) was obtained from Wako Pure Chemical Industries, Ltd., Osaka, Japan. Dansyl-L-asparagine (DNSA), 2-hydroxyl-5-nitrobenzyl bromide (I-Br) and diethyl pyrocarbonate (DEP) were purchased from the Sigma Chemical Co. (St Louis, MO, U.S.A.). Restriction enzymes, T4 polynucleotide kinase, calf intestinal alkaline phosphatase, a DNA ligation kit, TaKaRa EX *Taq* DNA polymerase and a site-directed mutagenesis kit (oligonucleotide-directed dual amber method) were obtained from Takara Shuzo Co., Ltd. (Kyoto, Japan). A DNA sequence kit was obtained from Perkin-Elmer Applied Biosystems (Tokyo, Japan). The *Pichia* Expression kit was purchased from Invitrogen.

All other chemicals were of analytical grade.

Esterase-like Activity Measurement

Procedures for Michaelis-Menten Equation Runs

The reaction was started by adding CS-866 in 100% acetonitrile (5 μl) to

DMD Fast Forward. Published on September 23, 2005 as DOI: 10.1124/dmd.105.006163
This article has not been copyedited and formatted. The final version may differ from this version.

preincubated HSA (120 μl, 75 μM), at a final concentration of 10 to 250 μM. Incubation proceeded for 10 min, and was terminated by adding 500 μl of acetonitrile to the incubation mixture. We have checked that 4 % acetonitrile has little effect on the reaction. After centrifugation for 1 min, a 30-μl aliquot of the deproteinized supernatant was subjected to HPLC, and RNH-6270 was separated from CS-866 on an ODS column using the following conditions: column, YMC-Pack ODS-AM, AM-302, 150 × 4.6 mm I.D; column temperature, 40ºC maintained by HITACHI 655A-52 Column Oven; pump, HITACHI L-6000 Pump; detector, HITACHI FL Detector L-7480 fluorescent monitor; integrator, HITACHI D-2500 Chromato-Integrator; mobile phase, acetonitrile: water: acetic acid = 40:60:0.1; wavelength, E_X=260 nm, E_M=370 nm; flow rate, 1.0 ml/min.

The reaction between CS-866 and HSA took place at 4 ºC. Under that condition, Michaelis-Menten equation analysis can be applied.

$$v = \frac{V_{max}[S]}{K_M + [S]} \quad (1)$$

Here, [S] is the concentration of substrate. That is the case, because previous studies have revealed a linear relationship between 1/*V* and 1/S when plotted in a Lineweaver-Burk plot (Koike et al., 2001):

$$\frac{1}{v} = \frac{1}{V_{max}} + \frac{K_M}{V_{max}[S]} \quad (2)$$

Procedures for Kinetic Runs

Hydrolysis of CS-866 (5 μM) by HSA (at least a 5-fold excess concentration over the substrate) was performed using conditions able to avoid complications due to

DMD Fast Forward. Published on September 23, 2005 as DOI: 10.1124/dmd.105.006163
This article has not been copyedited and formatted. The final version may differ from this version.

multiple reactive sites of albumin. Under such conditions, pseudo-first-order rate constant analysis can be performed. The pseudo-first-order rate constant for the release of RNH-6270 (k_{obs}), the dissociation constant of the substrate-HSA complex (K_S) and the catalytic rate constants (k_{cat}) were calculated as reported elsewhere (Sakurai et al., 2004).

Thermodynamic Analysis

Thermodynamic analysis of the HSA-catalyzed reaction was performed at temperatures ranging from 20ºC to 40ºC. We calculated the thermodynamic parameters, the free energy change for the initial reaction between enzyme and substrate (ΔG_S), the activation free energy for the rate-determining step (ΔG), the free energy difference for the reaction (ΔG_T), the activation energy (E_a), the activation enthalpy change (ΔH) and the activation entropy change (ΔS), using previously published methods (Sakurai et al., 2004).

Effects of Ligands

HSA (120 μl, 75 μM) was preincubated, and the enzymatic reaction was started by adding CS-866 in 100% acetonitrile (5 μl) to the solution, at a final concentration of 100 to 250 μM, in the presence or absence of each ligand (at a final concentration of 0-600 μM) (Ikeda, 2000). Incubation proceeded for 10 min at 37ºC, and the release of RNH-6270 was measured by HPLC as described above.

Chemical Modification of HSA

Histidine Residues

Chemical modification of His residues was performed using diethyl pyrocarbonate (DEP) (Roosemont, 1978). An average of 2.22 His residues was modified out of the total of 16 His residues.

Lysine Residues

Chemical modification of Lys residues was performed according to Gounaris and Perlmann (1967). The modification ratio was calculated as described by Haynes et al. (1967). An average of 3.80 out of the 59 Lys residues was modified.

Tyrosine Residues

Chemical modification of Tyr residues was performed as outlined by Sokolovsky et al. (1966). An average of 1.24 out of the 18 Tyr residues was modified.

Tryptophan Residues

Chemical modification of the single Trp residue was performed at room temperature (Fehske et al., 1978). An average of 0.88 out of the 1 Trp residue was modified.

Chemical modifications of specific amino acid residues (Tyr, Lys, His and Trp) were performed with the assumption that the effects on other amino acid residues would be negligible. The secondary and tertiary protein structures of all the modified HSAs were examined by circular dichroism (CD) measurements before use, and no significant difference was observed between the derivatives and native HSA (data not shown).

Synthesis and Purification of rHSA Forms

DMD Fast Forward. Published on September 23, 2005 as DOI: 10.1124/dmd.105.006163
This article has not been copyedited and formatted. The final version may differ from this version.

The recombinant DNA techniques used to produce wild-type rHSA and the single-residue mutants were essentially the same as those described by Watanabe et al. (2001). A chimaeric plasmid (pJDB-ADH-L10-HSA-A) containing cDNA for the mature form of HSA and an L10 leader sequence was donated by Tonen Co. (Tokyo, Japan). The mutagenic primers used (underlined letters indicate mismatches) were as follows:

5’-CAAACAGAGACTCGCCTGTGCCAGTCTCC-3’ for K199A;

5’-GAGCTTTCAAAGCAGCTGCAGTAGCTCGCCTG-3’ for W214A;

5’-CTATTAGTTCGTGCCACCAAG-3’ for Y411A.

The L10-HSA coding region was amplified by PCR using a forward and a reverse primer containing a 5’-terminal *Eco*RI site, and was cloned into the *Eco*RI-digested pKF19k vector (Takara Shuzo Co. Kyoto, Japan), and mutagenesis was then performed. The mutation was confirmed by DNA sequencing of the entire HSA coding region using the dideoxy chain termination method and a PerkinElmer ABI Prism 310 Genetic Analyzer. To construct the HSA expression vector pHIL-D2-HSA, an L10-HSA coding region with or without the desired mutation site was incorporated into the methanol-inducible pHIL-D2 vector (Invitrogen Co., San Diego, CA, U.S.A.). The resulting vector was introduced into the yeast species *Pichia pastoris* (strain GS115) to express rHSA. Secreted rHSA was isolated from the growth medium by precipitation with 60% ammonium sulphate at room temperature, and was then purified using a column of Blue Sepharose CL-6B (Amersham Pharmacia Co. Uppsala, Sweden). The eluted rHSA was deionized and then defatted using charcoal treatment.

The resulting protein exhibited a single band on an SDS/PAGE gel, and all of the recombinant proteins migrated to the same position as native HSA (data not shown).

Any secondary or tertiary structural differences between native (wild-type) and mutant rHSAs were analyzed by CD (data not shown). In the far-UV and near-UV regions, all rHSAs exhibited the same characteristics as native HSA.

Docking of CS-866 to HSA

In order to dock CS-866 to HSA, we used the crystal structure of the HSA:myristate:*S*-warfarin complex (PDB ID 1H9Z (Petitpas et al., 2001)). The docking calculation of CS-866 to HSA was performed using SYBYL FlexX (Rarey et al., 1996). CS-866 docked at site I and site II. The residues within 5 Å from *S*-warfarin were defined as site I, and the residues within 5 Å from myristate-3 and -4 were defined as site II. During the docking calculation, the structure of HSA was kept rigid. The docking algorithm generated 275 and 209 different placements of CS-866 in site I and site II, respectively. All placements were evaluated using the scoring function of FlexX. For each site, because the top 10 placements exhibited nearly identical binding modes, we chose the placement with the best value as the candidate binding mode.

Refinement of Docking Models

To refine the docking models, the coordinates of CS-866 and the residues within 10 Å from CS-866 were optimized to reduce the root mean square of the gradients of potential energy to below 0.05 kcal $mol^{-1}Å^{-1}$ using SYBYL 6.9.1 (Tripos, Inc., 2003). The Tripos force field was used for the molecular energy calculation. The AMBER 7 charges (Cornell et al., 1995) were used as the atomic charges for HSA. The Gasteiger-Hückel charges (Gasteiger and Marsili, 1980, 1981; Marsili and Gasteiger, 1980; Purcel and Singer, 1967) were used as the charges for CS-866. The cut-off

DMD Fast Forward. Published on September 23, 2005 as DOI: 10.1124/dmd.105.006163
This article has not been copyedited and formatted. The final version may differ from this version.

distance for the non-bonded interactions was 10 Å. The distance-dependent dielectric constant of 4r was used. Due to the lack of the 1st and 2nd *N*-terminal residues and the lack of the 585th *C*-terminal residue in the crystal structure of HSA, the 3rd and 584th residues were protected by an acetyl group and by an *N*-methyl group, respectively. The initial positions of the other missing atoms in the crystal structure were generated by SYBYL.

Statistics

Where possible, statistical analyses were performed using Student's *t* test.

DMD Fast Forward. Published on September 23, 2005 as DOI: 10.1124/dmd.105.006163
This article has not been copyedited and formatted. The final version may differ from this version.

Results

Hydrolytic Kinetics

First, we were able to confirm that the hydrolysis of CS-866 by HSA followed Michaelis-Menten kinetics (data not shown). Table 1 shows the K_M, V_{max}, k_{cat}, and the specificity constant (k_{cat}/K_M) values for the hydrolytic reaction.

To elucidate the reactivity of CS-866, we compared the kinetic parameters for CS-866 with those determined for the release of *p*-nitrophenol from PNPA (Table 2) (Means and Bender, 1975; Sakurai et al., 2004). The K_S value was found to be lower for CS-866, suggesting that PNPA has greater affinity than CS-866 for HSA (Sakurai et al., 2004; Fersht, 1998). The catalytic rate constant, k_{cat}, was also found to be greater for PNPA.

Thermodynamics

The relationship between the catalytic rate constants and temperature followed the Arrhenius equation. Accordingly, a linear relationship was found between ln k_{cat} and 1/T, where T is the absolute temperature in degrees K (data not shown). The activation energy of the reaction, E_a, calculated from the Arrhenius plot (Sakurai et al., 2004; Fersht, 1998), was found to be 37.1 $kJ \cdot mol^{-1}$.

Using the HSA-hydrolysis parameters, we compared energy changes and thermodynamic parameters between CS-866 and PNPA (Table 3). CS-866 had larger values of ΔG (96.3 $kJ \cdot mol^{-1}$) and ΔS (-0.207 $kJ \cdot mol^{-1} \cdot K^{-1}$) than PNPA.

Effects of Ligands on Hydrolysis

The site I-specific ligands warfarin, DNSA and n-butyl *p*-AB were used as

DMD Fast Forward. Published on September 23, 2005 as DOI: 10.1124/dmd.105.006163
This article has not been copyedited and formatted. The final version may differ from this version.

inhibitors to investigate for any competition with the hydrolytic reaction (Kragh-Hansen et al., 2002; Yamasaki et al., 1996). Interestingly, warfarin inhibited hydrolysis in a competitive manner, with a K_i value of 155 μM in a Dixon plot (Fig. 2A). By contrast, neither n-butyl *p*-AB nor DNSA inhibited HSA-catalyzed hydrolysis of CS-866 (Fig. 2B and 2C).

The site II-specific ligands ibuprofen and diazepam were used to investigate, whether there is competition between that ligand-binding site and the catalytic site (Kragh-Hansen et al., 2002). Diazepam had no inhibitory effect, but competitive inhibition was observed with ibuprofen, with a K_i value of 235 μM in a Dixon plot (Fig. 3A and 3B).

Effect of Chemical Modification on Hydrolysis

Hydrolytic activities of the 4 specifically modified HSA derivatives (Tyr-, Lys-, His- and Trp-HSA) were assayed (Fig. 4). Compared with native-type HSA, all modified HSA derivatives had significantly decreased hydrolytic activity ($p< 0.05$). Modification of Lys residues or of the single Trp residue resulted in the most pronounced reductions in catalytic reactivity.

Examination of Hydrolytic Activity Using Site-directed Mutagenesis

Wild-type rHSA and the HSA single-residue mutants K199A, W214A and Y411A were used to examine involvement of various amino acid residues in the hydrolysis. The hydrolytic activity of each rHSA was examined in order to elucidate the contribution of specific amino acid residues (Fig. 5). Compared with the wild-type rHSA, all mutant rHSAs showed significant decreases in catalytic activity. K199A exhibited a particularly

marked decrease in catalytic activity ($P < 0.001$), suggesting that Lys-199 plays a particularly important role in the hydrolysis. These results are in good agreement with those obtained with the chemically modified HSAs. The W214A and Y411A mutants showed a significant reduction in catalytic activity ($P < 0.05$), indicating that the amino acid residues Trp-214 and Tyr-411 are also involved in the hydrolytic reaction.

Molecular Interaction of CS-866 and HSA in Docking Models

We obtained 2 docking models: model I for site I, and model II for site II. In model I, the binding of CS-866 was similar to that of warfarin (Fig. 6). The biphenyl moiety of CS-866 was bound to the hydrophobic pocket consisting of Leu-219, Leu-238, Val-241, Leu-260, Ala-261, Ile-264, Ile-290, and Ala-291. The 2-propyl-imidazole moiety and the propan-2-ol moiety were bound to the other hydrophobic pocket (Phe-211, Trp-214, Ala-215, Leu-219, and Leu-238). Hydrogen bonds to and electrostatic interactions with other residues are detailed in Table 4. Oxygen atoms of the vinylene carbonate moiety formed hydrogen bonds with side chains of Arg-218 and of Arg-222. Negative charges of the tetrazole moiety interacted electrostatically with side chains of Lys-199 and of Arg-257. The hydroxyl oxygen atom of the propan-2-ol moiety formed a hydrogen bond with the side chain of Lys-199, and the hydrogen atom formed a hydrogen bond with the side chain of His-242. The carbonyl oxygen atom of the ester moiety formed a hydrogen bond with the side chain of Lys-199. The ester moiety of CS-866 was in the vicinity of Glu-292. However, the side chain of Glu-292 was distant from the carbonyl carbon of the ester moiety, because the docking program, FlexX, cannot account for chemical reactions and remains rigid. We changed the torsion angles of the side chain of Glu-292 without steric hindrance as Glu-292 became capable of a nucleophilic reaction.

In model II, CS-866 was bound to site II using the pocket for myristate-4 (Fig. 7) (Curry et al., 1998). The pocket for myristate-3 was not occupied. The biphenyl moiety and the 2-propyl-imidazole moiety were bound to the hydrophobic pocket consisting of Leu-387, Pro-486 and Ala-490. The propan-2-ol moiety was surrounded by the hydrophobic residues (Leu-387, Leu-430 and Leu-453). Table 5 shows hydrogen bonds and electrostatic interactions in site II. Negative charges of the tetrazole moiety interacted electrostatically with the side chain of Arg-485, and the tetrazole moiety formed a hydrogen bond with the side chain of Asn-391. The side chain of Ser-489 formed hydrogen bonds with the hydroxyl oxygen atom of the propan-2-ol moiety and the carboxyl oxygen atom of the ester moiety. The carbonyl oxygen atom of the ester moiety formed a hydrogen bond with the side chain of Lys-414. The carboxyl oxygen atom of the ester moiety formed a hydrogen bond with the side chain of Tyr-411.

Discussion

This antihypertensive prodrug, CS-866, is hydrolyzed in the serum. Hydrolysis of CS-866 in serum has been observed in several species, and comparison between 5 species has shown that hydrolytic activity is highest in rabbits, followed by dogs, mice, rats and humans (Ikeda et al., 2000). Furthermore, we examined the activity due to serum albumin. It was found to be highest in humans, followed by rats, mice, rabbits and dogs (data not shown). This indicates that the mechanisms of hydrolysis of CS-866 in serum differ among those species, and that HSA plays a more important role in producing RNH-6270 than other serum albumin species.

Thermodynamic Properties

The esterase-like activity of HSA is dependent on the catalytic rate constant, k_{cat}, and increases with a decrease in the activation free energy change, ΔG. Thus, the magnitude of ΔG, which is dependent on activation entropy change (ΔS), as calculated from a thermodynamic analysis, can be regarded as an indicator of hydrolytic activity of HSA (Sakurai et al., 2004; Fersht, 1998). Because PNPA has lower ΔG and ΔS values than CS-866 (Table 3), PNPA exhibited greater affinity for HSA and a higher catalytic rate than CS-866 (Table 2). Hydrolysis reactions catalyzed by albumin have previously been found to have a particularly great entropy difference between the ground state (ES) and the transition state (ES*) (Sakurai et al., 2004). The active sites of HSA to which the substrate binds is perfectly oriented to the reactive site of the substrate (the ester portion) for hydrolysis, and thus has a smaller entropy difference between the transition state (ES*) and the ground state (ES). This may be the reason why hydrolysis of PNPA proceeds more readily than hydrolysis of CS-866. That is, compared to CS-866, PNPA

has a structure and orientation that are better suited to hydrolysis by HSA.

Relationship Between Ligand Binding Sites and Hydrolytic Active Sites

HSA is the most abundant protein in blood plasma, and serves as a storage protein and transport protein for many endogenous and exogenous compounds (Kragh-Hansen et al., 2002; Peters, 1996). The unique capability of HSA to reversibly bind a large number of compounds is usually explained by the existence of a number of binding regions (including site I and site II), each of which has a very different specificity (Kragh-Hansen et al., 2002; Kragh-Hansen, 1991). Furthermore, site I on HSA consists of 3 subsites: Ia, Ib and Ic (Fehske et al., 1982; Yamasaki et al., 1996). Another important role of HSA is as a catalyst for the hydrolysis of various compounds, such as esters, amides and phosphates. It has been suggested that the active site of HSA for *p*-nitrophenyl esters is site II, and that Tyr-411 is essential for hydrolysis of *p*-nitrophenyl esters (Ozeki et al., 1980; Watanabe et al., 2000). The reactive site and active residue for nitroaspirin are reportedly site I and Lys-199, respectively (Ikeda and Kurono, 1986). The relationship between the hydrolytic active sites of HSA for CS-866 and the proteins ligand-binding sites was investigated in the present study.

There are interesting patterns of competition between site-I and site-II ligands for hydrolysis. Although warfarin, which is regarded as a typical ligand of subsite Ia of HSA, acts as a competitive inhibitor, this does not necessarily indicate that the HSA catalytic site for CS-866 is subsite Ia, because ibuprofen, a typical site II ligand, also exhibited evidence of competitive inhibition (Fig. 2A and 3B). These results suggest that substrate specificity of the esterase-like region and ligand-binding site of HSA is inconsistent. In other words, the catalytic site for CS-866 on HSA may recognize

CS-866 in a manner different from that of the ligand-binding site.

Roles of Specific Amino Acid Residues

For proteins whose X-ray crystallographic structure is known, the role of each amino acid residue can be quantitatively determined using the amino acid displacement (site-directed mutagenesis) technique and information obtained from X-ray analysis.

The present chemical modification experiments indicate that Lys, Trp and Tyr residues of HSA are important for hydrolysis of CS-866 by HSA, and that His residues are also involved (Fig. 4). These experiments were performed with mildly modified HSA, because, for example, only 1.24 of the Tyr residues and 3.8 of the Lys residues were modified. However, HSA has 59 Lys residues, and the numbers of Trp, Tyr and His residues are 1, 18 and 16, respectively. Previous findings have demonstrated that Tyr-411 is most likely the reactive Tyr of HSA (Watanabe et al., 2000). It is also known that the reactivity of Lys-199 is high (Means and Bender, 1975). Further, it is reported that this single Trp residue contributes to the esterase-like activity of HSA (Ozeki et al., 1980; Kurono et al., 1982). In an attempt to identify specific residues of importance for the hydrolysis of CS-866, we examined the activity of several rHSAs, namely wild-type HSA and the single-residue mutants K199A, W214A and Y411A.

Because we did not observe great decrease of the hydrolytic activity of HSA for CS-866, even in the single-residue mutants K199A and Y411A, we conclude that the catalytic sites of HSA for CS-866 are not solely confined to the Lys-199 and Tyr-411 residues, but rather involves several additional amino acid residues (Fig. 5).

The single Trp residue, Trp-214, is located close to Lys-199, as indicated by X-ray diffraction analysis, and is an element of a major interdomain cluster of hydrophobic

residues (Sugio et al., 1999; He and Carter, 1992). The mutant W214A exhibited a significant decrease in hydrolytic activity (Fig. 5). In addition, the microenvironment near Trp-214 was investigated to obtain detailed information about the role of this residue in the hydrolysis. After incubation with CS-866 for 10 minutes, the relative fluorescence intensity of HSA decreased by more than half and the λ_{max} was blue-shifted (data not shown). These results are consistent with a model indicating that the Trp-214 residue is involved in hydrolytic reaction. These limited data leads us the idea that a double (or triple) mutation of Lys-199, Trp-214 and Tyr-411 could completely abolish the hydrolytic activity. Further investigations on this point are under way at this laboratory.

Structural Mechanism of Hydrolysis Based on Models

The present findings suggest that HSA has 2 catalytic sites for CS-866, for the following 2 reasons. Mutation at site I or site II diminishes but does not abolish the hydrolytic activity. The hydrolytic activity is inhibited by both warfarin (site I drug) and ibuprofen (site II drug).

In model I (Fig. 6), CS-866 occupied the binding site of warfarin; this is consistent with the results showing that warfarin inhibits the hydrolytic activity of HSA. In site I, the carbonyl oxygen atom of the ester moiety formed a hydrogen bond with the side chain of Lys-199, and this hydrogen bond could function as an oxyanion hole. The importance of Lys-199 indicated by the model is consistent with the decreased hydrolytic activity of the K199A mutant and the HSA variant produced by chemical modification of Lys. The catalytic residue may be Glu-292; the distance between the oxygen atom of the side chain of Glu-292 and the carbonyl carbon of the ester moiety of

CS-866 was 4.8 Å. The hydrophobic interaction between CS-866 and Trp-214 indicated by the model is consistent with the diminished hydrolytic activity of the W214A mutant and the HSA variant produced by chemical modification of Trp.

Model II (Fig. 7) indicates that the mechanism of hydrolysis of CS-866 is almost the same as that found in previous studies for *p*-nitrophenyl esters, with the exception of the involvement of Arg-410 (Sakurai et al., 2004; Watanabe et al., 2000). Instead of Arg-410, Lys-414 was used to create an oxyanion hole. The distance between the hydroxyl oxygen atom of Tyr-411 and the carbonyl carbon of the ester moiety of CS-866 was 3.3 Å, indicating that it is possible that Tyr-411 plays the role of a cathartic residue. The importance of Tyr-411 and Lys-414 is consistent with the decreased hydrolytic activity of the Y411A mutant and of the HSA variants produced by chemical modification of Tyr or Lys. In our model II, CS-866 was bound to the pocket for myristate-4 in site II. The binding pockets of the site II ligands ibuprofen and diazepam are unknown. If ibuprofen binds to the pocket for myristate-4, our model II provides a mechanism for inhibition of hydrolytic activity of HSA by ibuprofen.

The present findings indicate that hydrolysis of CS-866 by HSA is dependent on ΔS. Another important factor is the orientation between the catalytic active site on HSA and the ester region of the substrate. There are differences between the catalytic active sites and the ligand-binding sites of HSA. Furthermore, the residues of Lys-199, Trp-214 and Tyr-411 play important roles in this catalytic reaction. All of these experimental findings are consistent with the docking model that we derived from computer simulation.

Acknowledgments

This work was supported in part by Grant-in-Aid for scientific research from the Ministry of Education, Science and Culture of Japan (11694298 for M.O.) and was also supported in part by Grant-in-Aid for scientific research, encouragement of young scientists (B) (13771414 for N.Y.) from Japan Society for the Promotion of Science.

References

Brousil JA and Burke JM (2003) Olmesartan medoxomil: an angiotensin II-receptor blocker. *Clin Ther* **25:** 1041-1055.

Chen RF (1967) Removal of fatty acids from serum albumin by charcoal treatment. *J Biol Chem* **242:** 173-181.

Curry S, Mandelkow H, Brick P and Franks N (1998) Crystal structure of human serum albumin complexed with fatty acid reveals an asymmetric distribution of binding sites. *Nat Struct Biol* **5**:827-835.

Cornell WD, Cieplak P, Bayly CI, Gould IR, Merz KM Jr, Ferguson DM, Spellmeyer DC, Fox T, Caldwell JW and Kollman PA (1995) A second generation force field for the simulation of proteins, nucleic acids, and organic molecules. *J Am Chem Soc* **117**:5179-5197.

Fehske KJ, Müller WE and Wollert U (1978) The modification of the lone tryptophan residue in human serum albumin by 2-hydroxy-5-nitrobenzyl bromide. Characterization of the modified protein and the binding of L-tryptophan and benzodiazepines to the tryptophan-modified albumin. *Hoppe-Seylers Z Physiol Chem* **359:** 709-717.

Fehske KJ, Schläfer U, Wollert U and Müller WE (1982) Characterization of an important drug binding area on human serum albumin including the high-affinity binding sites of warfarin and azapropazone. *Mol Pharmacol* **21:** 387-393.

Fersht A (1998) *Structure and Mechanism in Protein Science,* Freeman, New York.

Gasteiger J and Marsili M (1980) Iterative partial equalization of orbital electronegativity: a rapid access to atomic charges. Tetrahedron 36:3219-3228.

Gasteiger J and Marsili M (1981) Prediction of proton magnetic resonance shifts: the dependence on hydrogen charges obtained by iterative partial equalization of orbital

electronegativity. *Organ Magn Reson* **15**:353-360.

Gounaris AD and Perlmann GE (1967) Succinylation of pepsinogen. *J Biol Chem* **242:** 2739-2745.

Haynes R, Osuga DT and Feeney RE (1967) Modification of amino groups in inhibitors of proteolytic enzymes. *Biochemistry* **6:** 541-547.

He XM and Carter DC (1992) Atomic structure and chemistry of human serum albumin. *Nature* **358:** 209-215.

Ikeda K and Kurono Y (1986) Enzymatic activity and drug binding activity of human serum albumin. *Yakugaku Zasshi* **106:** 841-855.

Ikeda T (2000) Two prodrugs activated by serum esterases including albumin. Proceedings of the international symposium on Serum Albumin & α_1-Acid Glycoprotein 173-180.

Koike H, Sada T and Mizuno M (2001) In vitro and in vivo pharmacology of olmesartan medoxomil, an angiotensin II type AT1 receptor antagonist. *J Hypertens Suppl* **19:** 1:S3-14.

Kragh-Hansen U (1991) Octanoate binding to the indole- and benzodiazepine-binding region of human serum albumin. *Biochem J* **273:** 641-644.

Kragh-Hansen U, Chuang VTG and Otagiri M (2002) Practical aspects of the ligand-binding and enzymatic properties of human serum albumin. *Biol Pharm Bull* **25:** 695-704.

Kurono Y, Yamada H and Ikeda K (1982) Effects of drug binding on the esterase-like activity of human serum albumin. V. Reactive site towards substituted aspirins. *Chem Pharm Bull* **30:** 296-301.

Marsili M and Gasteiger J (1980) Pi-Charge Distributions from Molecular Topology and

Pi-Orbital Electronegativity. *Croat Chem Acta* **53**:601-614.

Means GE and Bender ML (1975) Acetylation of human serum albumin by p-nitrophenyl acetate. *Biochemistry* **14:** 4989-4994.

Neutel JM (2001) Clinical Studies of CS-866, the newest angiotensin II receptor antagonist. *Am J Cardiol* **87 (8A):** 37C-43C.

Ozeki Y, Kurono Y, Yotsuyanagi T and Ikeda K (1980) Effects of drug binding on the esterase activity of human serum albumin: inhibition modes and binding sites of anionic drugs. *Chem Pharm Bull* **28:** 535-540.

Peters T Jr (1996) *All about albumin, Biochemistry, Genetics, and Medical Applications*, Academic Press, San Diego.

Petitpas I, Bhattacharya AA, Twine S, East M and Curry S (2001) Crystal structure analysis warfarin binding to human serum albumin: anatomy of drug site I. *J Biol Chem* **276**:22804-22809.

Purcel WP and Singer JA (1967) A brief review and table of semiempirical parameters used in the Hüeckel molecular orbital method. *J Chem Eng Data* **12**:235-246.

Rarey M, Kramer B, Lengauer T and Klebe G (1996) A fast flexible docking method using incremental construction algorithm. *J Mol Biol* **261**:470-489.

Roosemont JL (1978) Reaction of histidine residues in proteins with diethylpyrocarbonate: differential molar absorptivities and reactivities. *Anal Biochem* **88:** 314-320.

Sakurai Y, Ma SF, Watanabe H, Yamaotsu N, Hirono S, Kurono Y, Kragh-Hansen U and Otagiri M (2004) Esterase-like activity of serum albumin: characterization of its structural chemistry using p-nitrophenyl esters as substrates. *Pharm Res* **21:** 285-292.

Sokolovsky M, Riordan JF and Vallee BL (1966) Tetranitromethane. A reagent for the

nitration of tyrosyl residues in proteins. *Biochemistry* **5:** 3582-3589.

Sugio S, Kashima A, Mochizuki S, Noda M and Kobayashi K (1999) Crystal structure of human serum albumin at 2.5 A resolution. *Protein Eng* **12:** 439-446.

Watanabe H, Tanase S, Nakajou K, Maruyama T, Kragh-Hansen U and Otagiri M (2000) Role of Arg-410 and Tyr-411 in human serum albumin for ligand binding and esterase-like activity. *Biochem J* **349:** 813-819.

Watanabe H, Yamasaki K, Kragh-Hansen U, Tanase S, Harada K, Suenaga A and Otagiri M (2001) In vitro and in vivo properties of recombinant human serum albumin from Pichia pastoris purified by a method of short processing time. *Pharm Res* **18:** 1775-1781.

Yamasaki K, Maruyama T, Kragh-Hansen U and Otagiri M (1996) Characterization of site I on human serum albumin: concept about the structure of a drug binding site. *Biochim Biophys Acta* **1295:** 147-157.

DMD Fast Forward. Published on September 23, 2005 as DOI: 10.1124/dmd.105.006163
This article has not been copyedited and formatted. The final version may differ from this version.

Figure legends

Fig. 1 Hydrolysis of CS-866 to RNH-6270

Fig. 2 Effect of warfarin (A), n-butyl *p*-AB (B) and DNSA (C) (0~600 μM) on the hydrolysis of CS-866 by HSA

Reaction conditions: 75 μM HSA; 100-250 μM CS-866; 1/15 M phosphate buffer (pH 7.4); 37 ºC. Plots represent mean ± S.D. (n=3)

Fig. 3 Effect of diazepam (A) and ibuprofen (B) (0~600 μM) on the hydrolysis of CS-866 by HSA

Reaction conditions: 75 μM HSA; 100-250 μM CS-866; 1/15 M phosphate buffer (pH 7.4); 37 ºC. Plots represent mean ± S.D. (n=3)

Fig. 4 Hydrolytic activities of chemically modified HSAs as compared with that of normal HSA

Reaction conditions: 75 μM HSA; 250 μM CS-866; 1/15 M phosphate buffer (pH 7.4); 37 ºC. Each column represents mean ± S.D. (n=3)

Significantly different from native type HSA ($p < 0.05$)

Fig. 5 Hydrolytic activities of mutant rHSAs as compared with that of wild type rHSA

Reaction conditions: 75 μM HSA; 250 μM CS-866; 1/15 M phosphate buffer (pH 7.4); 37 ºC. Each column represents mean ± S.D. (n=3)

# $p < 0.05$ and ## $p < 0.001$ as compared with wild type rHSA.

Fig. 6 Stereo drawings of ligands in site I: A) modeling structure for CS-866. The torsion angles of the side chain of Glu-292 were changed as Glu-292 becomes capable of a nucleophilic reaction, B) crystal structure for *S*-warfarin (PDB ID 1H9Z)
Relaxed stereo viewing.

Fig. 7 Stereo drawings of ligands in site II: A) modeling structure for CS-866, B) crystal structure for myristate-3 and -4 (PDB ID 1H9Z)
Relaxed stereo viewing.

DMD Fast Forward. Published on September 23, 2005 as DOI: 10.1124/dmd.105.006163
This article has not been copyedited and formatted. The final version may differ from this version.

Table 1 Kinetic parameters for the hydrolytic reaction between CS-866 and HSA at pH 7.4 and 37 ºC

HSA type	K_M (μM)	V_{max} (nmol·min^{-1})	k_{cat} (min^{-1})	k_{cat}/K_M (μM^{-1}·min^{-1})
native	48.2	1.02	0.113	0.00232

Reaction conditions: 75 μM HSA; 10-250 μM CS-866; 1/15 M phosphate buffer (pH 7.4); 37 ºC.

DMD Fast Forward. Published on September 23, 2005 as DOI: 10.1124/dmd.105.006163
This article has not been copyedited and formatted. The final version may differ from this version.

Table 2 Kinetic parameters for the hydrolysis of CS-866 and PNPA * by HSA at pH 7.4 and 25 ºC

Substrate	k_{cat} (10^{-3} ·sec^{-1})	K_S (μM)	k_{cat}/K_S (M^{-1} ·sec^{-1})
CS-866	0.845	42.5	19.9
PNPA*	86.8	217	403.4

PNPA*: data from Sakurai et al. (2004).

DMD Fast Forward. Published on September 23, 2005 as DOI: 10.1124/dmd.105.006163
This article has not been copyedited and formatted. The final version may differ from this version.

Table 3 Thermodynamic parameters for the hydrolysis of CS-866 and PNPA* by HSA

Substrate	ΔG_T ($kJ \cdot mol^{-1}$)	ΔG_S ($kJ \cdot mol^{-1}$)	ΔG ($kJ \cdot mol^{-1}$)	ΔH ($kJ \cdot mol^{-1}$)	ΔS ($kJ \cdot mol^{-1} \cdot K^{-1}$)
CS-866	71.3	-25.0	96.3	34.7	-0.207
PNPA*	58.1	-20.9	79.0	66.1	-0.0435

ΔG_T, free energy differences; ΔG_S, free energy change for the initial reaction of albumin and substrate; ΔG, activation free energy; ΔH, activation enthalpy change; ΔS, activation entropy change

Reaction conditions: 1/15 M phosphate buffer (pH 7.4), 25 ºC.

PNPA*: data from Sakurai et al. (2004).

DMD Fast Forward. Published on September 23, 2005 as DOI: 10.1124/dmd.105.006163
This article has not been copyedited and formatted. The final version may differ from this version.

Table 4 Hydrogen bonds and electrostatic interactions in model I of HSA:CS-866 complex

Hydrogen bonds				
Donor		Acceptor		Distance (Å)
Lys-199	N_ζ	Ester	C=O	4.1
	N_ζ	Propan-2-ol	OH	3.0
Propan-2-ol	OH	His-242	Nε2	4.6
Arg-218	N_ε	Vinylene carbonate	O2	3.8
	$N_\eta 2$		C=O	3.4
Arg-222	$N_\eta 2$		C1	3.1
Electrostatic Interactions				
Positive		Negative		Distance (Å)
Lys-199	N_ζ	Tetrazole	N2	5.7
Arg-257	N_ε		N4	2.8

DMD Fast Forward. Published on September 23, 2005 as DOI: 10.1124/dmd.105.006163
This article has not been copyedited and formatted. The final version may differ from this version.

Table 5 Hydrogen bonds and electrostatic interactions in model II of HSA:CS-866 complex

Hydrogen bonds				
Donor		Acceptor		Distance (Å)
Asn-391	$N_{\delta}2$	Tetrazole	N2	2.9
Tyr-411	O_{η}	Ester	-O-	2.8
Lys-414	N_{η}		C=O	2.7
Ser-489	O_{γ}		-O-	4.7
	O_{γ}	Propan-2-ol	OH	4.1
Electrostatic Interactions				
Positive		Negative		Distance (Å)
Arg-485	$N_{\eta}1$	Tetrazole	N3	3.5

DMD Fast Forward. Published on September 23, 2005 as DOI: 10.1124/dmd.105.006163
This article has not been copyedited and formatted. The final version may differ from this version.

Fig. 1

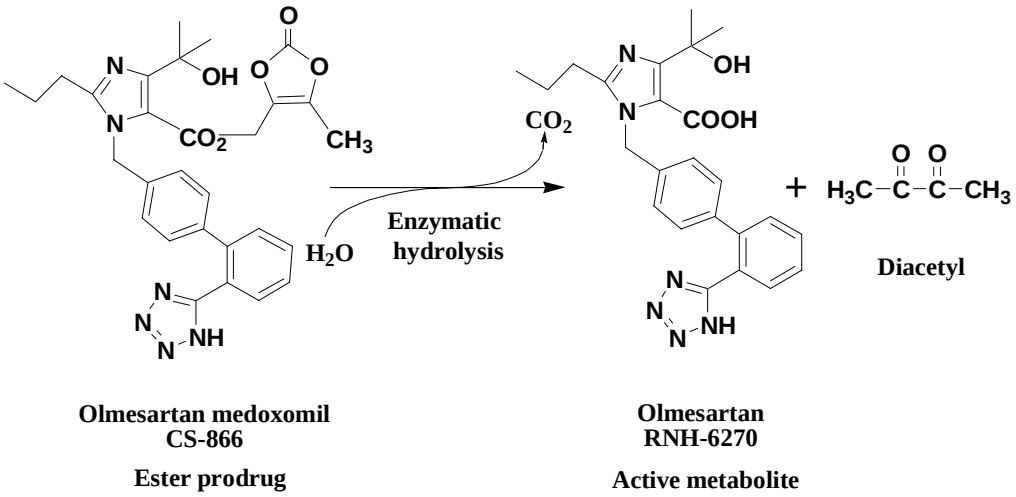

Olmesartan medoxomil
CS-866
Ester prodrug

Olmesartan
RNH-6270
Active metabolite

DMD Fast Forward. Published on September 23, 2005 as DOI: 10.1124/dmd.105.006163
This article has not been copyedited and formatted. The final version may differ from this version.

Fig. 2

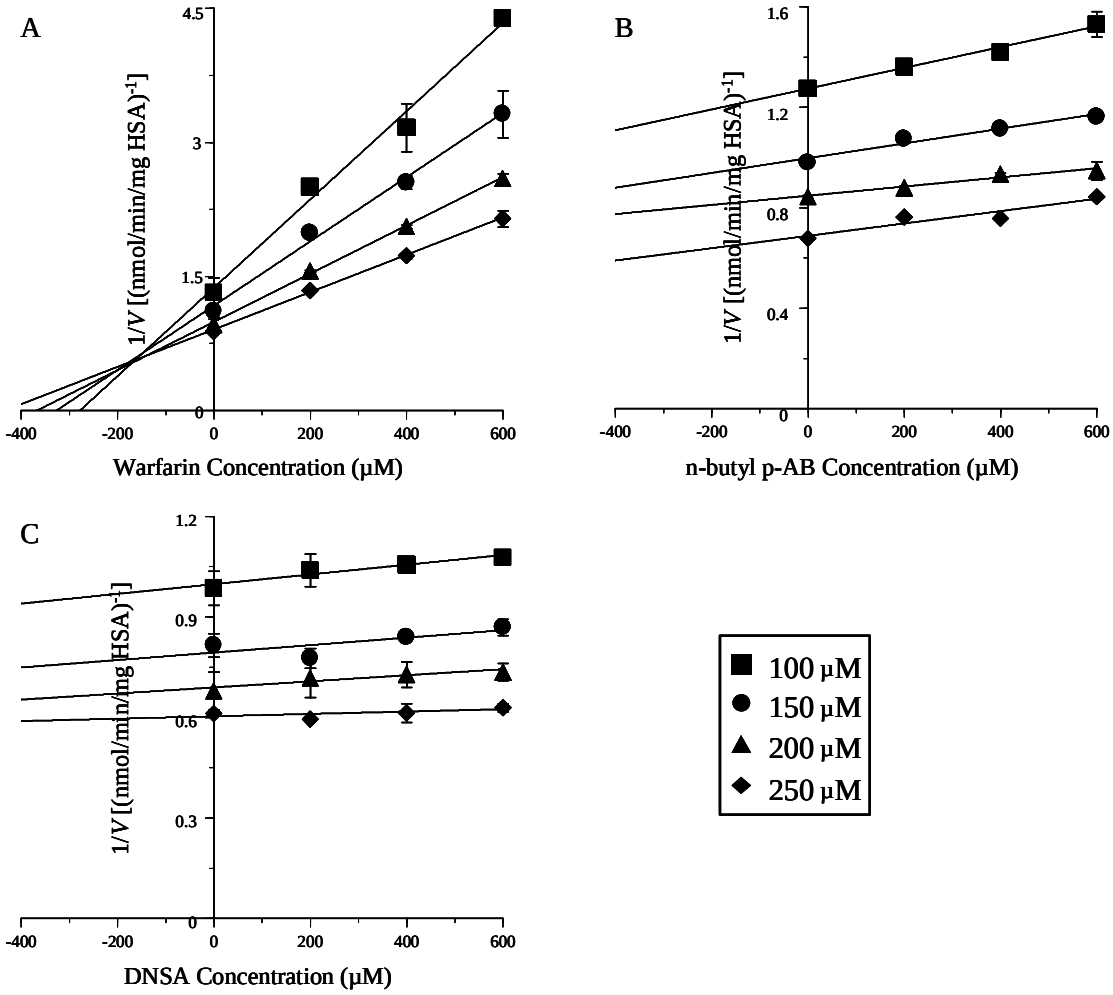

DMD Fast Forward. Published on September 23, 2005 as DOI: 10.1124/dmd.105.006163
This article has not been copyedited and formatted. The final version may differ from this version.

Fig. 3

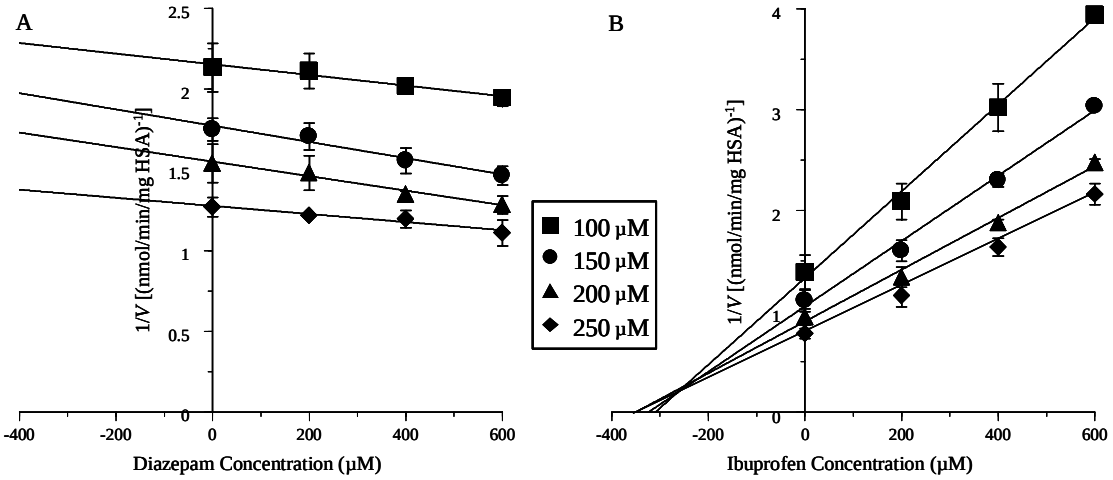

DMD Fast Forward. Published on September 23, 2005 as DOI: 10.1124/dmd.105.006163
This article has not been copyedited and formatted. The final version may differ from this version.

Fig. 4

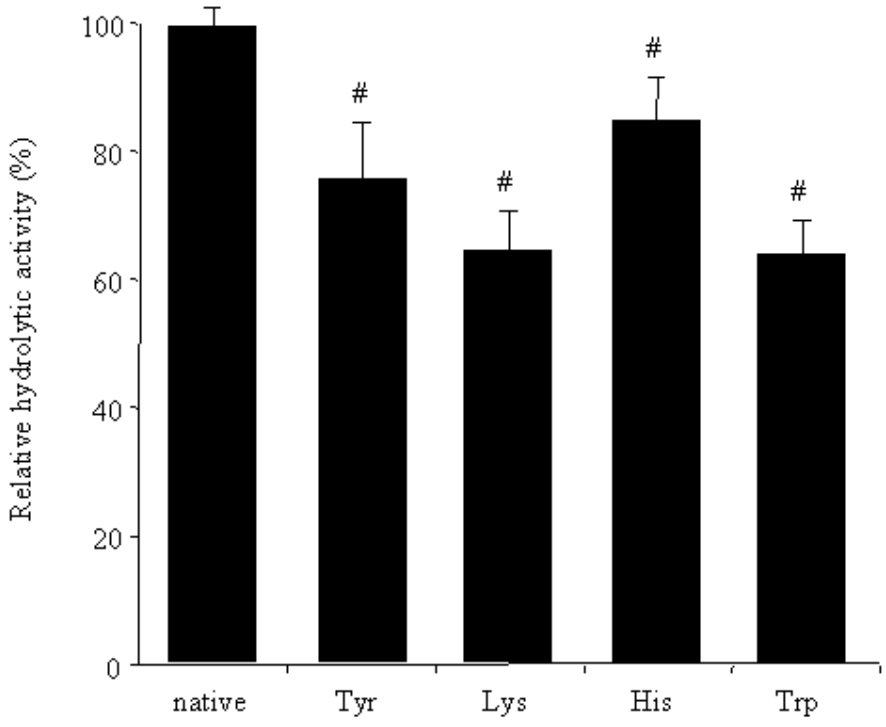

DMD Fast Forward. Published on September 23, 2005 as DOI: 10.1124/dmd.105.006163

Fig. 5

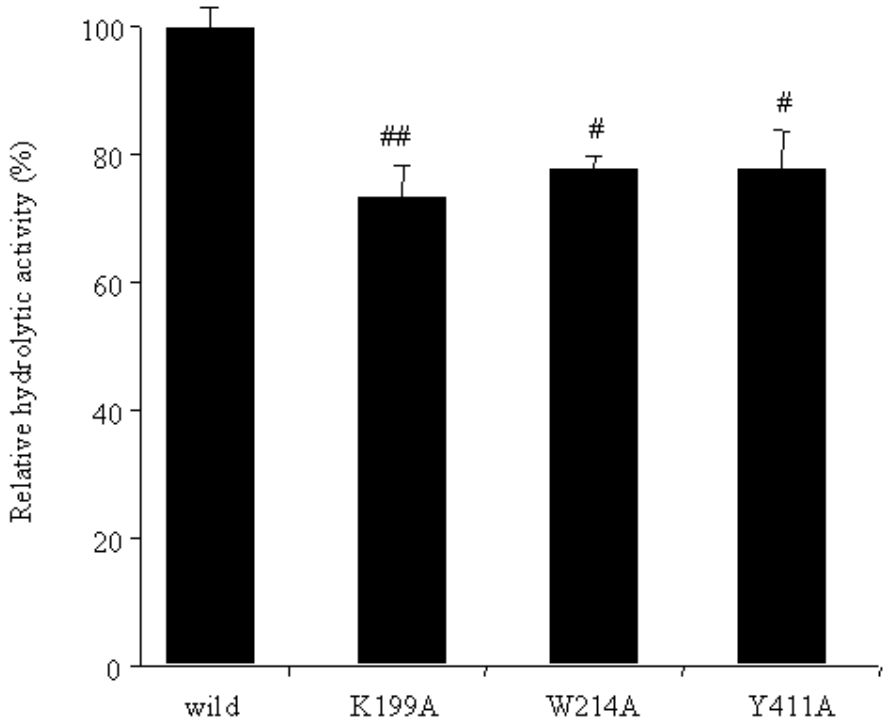

DMD Fast Forward. Published on September 23, 2005 as DOI: 10.1124/dmd.105.006163
This article has not been copyedited and formatted. The final version may differ from this version.

Fig. 6

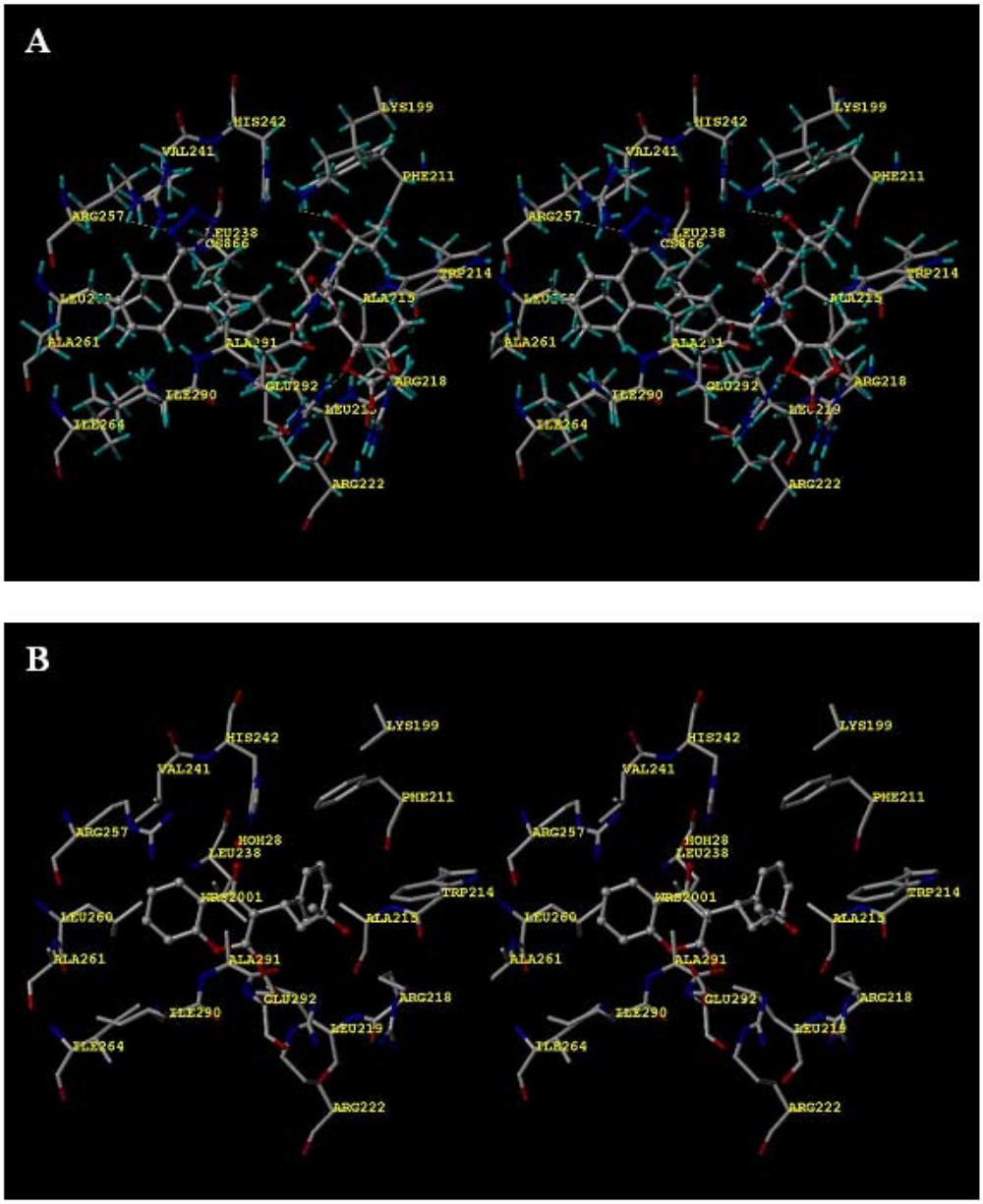

DMD Fast Forward. Published on September 23, 2005 as DOI: 10.1124/dmd.105.006163
This article has not been copyedited and formatted. The final version may differ from this version.

Fig. 7